

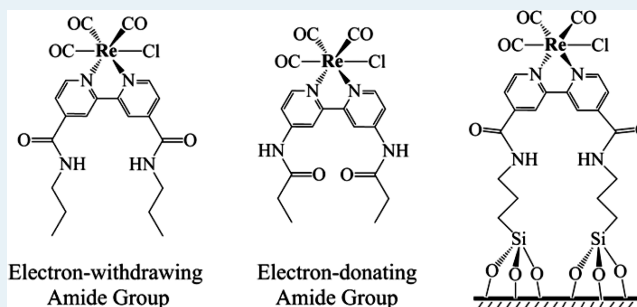
Photocatalytic CO₂ Reduction and Surface Immobilization of a Tricarbonyl Re(I) Compound Modified with Amide Groups

Chao Liu, Kevin D. Dubois, Michael E. Louis, Alexander S. Vorushilov, and Gonghu Li*

Department of Chemistry and Materials Science Program, University of New Hampshire, Durham, New Hampshire 03824, United States

ABSTRACT: Amide bonds have been utilized as covalent linkages between photosensitizers and molecular catalysts in some supramolecular photocatalysts. It is unclear how the presence of amide groups affects properties of the molecular catalysts. This study examines the effect of amide derivatization on photocatalytic CO₂ reduction using Re(bpy)(CO)₃Cl, where bpy is 2,2'-bipyridine. Our results indicate that derivatization with electron-withdrawing amide (–CONH) groups lowered the catalytic activity by a factor of ~6 when the Re(I) compound was directly excited in the absence of additional photosensitizers but facilitated electron transfer between Ru(bpy)₃²⁺ and the Re(I) catalyst when Ru(bpy)₃²⁺ was used as a photosensitizer for excited-state electron transfer. The electron-withdrawing amide bond was then utilized to graft the Re(I) complex onto the surface of silica nanoparticles. The surface Re(I) sites were found to be well separated in a diimine-tricarbonyl coordination environment. The surface-immobilized catalyst showed activity comparable to the homogeneous Re(I) compound in photocatalytic CO₂ reduction. Photochemical properties of the surface Re(I) catalyst were further probed using in situ FTIR and EPR spectroscopies. In the presence of a sacrificial electron donor, bipyridine-based, one-electron reduction of the surface Re(I) catalyst occurred upon visible-light irradiation. The results are particularly relevant to the development of photoelectrochemical devices for sustainable fuel production via CO₂ reduction.

KEYWORDS: rhenium, photocatalysis, CO₂ reduction, amide linkage, surface immobilization



1. INTRODUCTION

Developing methods to recycle CO₂ in a sustainable manner is an extremely active research topic.^{1,2} Photocatalytic CO₂ reduction is a promising long-term solution to CO₂ utilization that employs sunlight as a renewable energy input.^{3–5} Wide-bandgap semiconductors, such as titanium dioxide nanomaterials,^{6–8} have been widely investigated as robust photocatalysts for CO₂-to-fuel conversion. Transition metal compounds, including those of Ru and Re, are homogeneous catalysts capable of mediating multielectron CO₂ reduction.^{9–11} Tricarbonyl Re compounds have been studied as a model catalyst for electrocatalytic and photocatalytic CO₂ reduction since the early report by Hawecker et al.¹² The photophysical and photochemical properties as well as catalytic reactivity of tricarbonyl Re(I) complexes can be significantly altered by modifying or derivatizing ligands of the Re(I) metal center.^{13–16}

Many molecular and supramolecular systems have utilized amide groups as covalent linkages to facilitate electron transfer between electron donating components and reactive centers.^{17–23} For example, tricarbonyl Re(I) complexes were covalently linked to metalloporphyrins via amide moieties to form supramolecular photocatalysts, in which the C atom of the amide group was directly attached to the Re(I) complexes.^{17–19} In a different study, a tricarbonyl Re(I) complex was covalently

linked to a zinc porphyrin, forming a supramolecular photocatalyst bearing an amide group with the N atom connected to the Re(I) complex.²⁰ Such heteronuclear dyads can absorb long-wavelength light for photoinduced intramolecular electron transfer. Our recent study demonstrated that derivatization of the Re(I) catalyst with amide groups led to a red shift of the metal-to-ligand charge transfer (MLCT) band of Re(bpy)(CO)₃Cl, where bpy is 2,2'-bipyridine.²⁴ It is unclear, however, how derivatization of the bpy ligands with amide groups affects photocatalytic properties of the Re(I) complexes. This present work examines the effect of amide derivatization on photocatalytic CO₂ reduction using Re(bpy)(CO)₃Cl.

Furthermore, the amide groups are employed as linking moieties to immobilize the Re(I) complex on a solid-state surface via a new method. Covalent attachment of molecular catalysts on electrode surfaces is a viable approach to fabricate devices for photoelectrochemical CO₂ reduction,^{25–27} which eliminates the need for sacrificial electron donors and expensive molecular photosensitizers. The design and synthesis of covalent linkages plays a key role in successful fabrication of

Received: December 10, 2012

Revised: February 21, 2013

Published: February 25, 2013

photoelectrochemical devices for CO₂-to-fuel conversion. Our research involves the investigation of various surfaces and linking strategies for robust surface attachment of molecular catalysts. This present study employs a commercially available fumed silica as an inert support for tricarbonyl Re(I) complexes. A Re(I) complex was covalently attached to the silica surface, characterized with spectroscopic techniques, and compared against the corresponding homogeneous complexes in photocatalytic CO₂ reduction in the presence of a sacrificial electron donor.

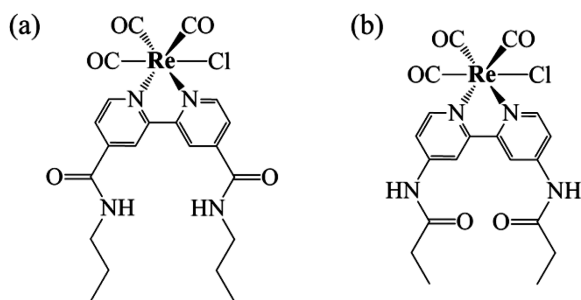
Finally, photochemical reduction of the surface-immobilized Re(I) catalyst in solid state was investigated with in situ spectroscopic techniques, including Fourier transform infrared (FTIR) and electron paramagnetic resonance (EPR) spectroscopies. The in situ spectroscopic studies provided useful information on the structural and functional properties of the surface Re(I) sites.

2. EXPERIMENTAL METHODS

2.1. Materials. Thionyl chloride, 2,2'-bipyridine-4,4'-dicarboxylic acid, propylamine, triethylamine (TEA), triethanolamine (TEOA), dichloromethane (DCM), dimethylformamide (DMF), tetrabutylammonium hexafluorophosphate (TBAH, ≥99%), 3-aminopropyltrimethoxysilane (APTMS), pentacarbonyl chlororhenium(I), and tris(2,2'-bipyridine) dichlororuthenium(II) hexahydrate (denoted "Ru(bpy)₃²⁺") were obtained from Sigma-Aldrich. 4,4'-Diamino-2,2'-bipyridine was obtained from BOC Sciences. All reagents were used without further purification. A nonporous fumed silica (Aerosil 200) obtained from Evonik was used as the model substrate for surface immobilization.

2.2. Synthesis and Characterization of Homogeneous Re(I) Catalysts. Three homogeneous Re(I) compounds were synthesized in this study. The synthesis of Re(bpy)(CO)₃Cl (denoted Re-bpy) and a Re(I) compound derivatized with amide groups (Re-L1, see Scheme 1a) was reported in our

Scheme 1. Molecular Structures of (a) Re-L1 and (b) Re-L2



recent study.²⁴ The synthesis of another derivatized Re(I) compound (Re-L2, see Scheme 1b) started with the preparation of 4,4'-dipropionylamido-2,2'-bipyridyl. Initially, 50 mg of 4,4'-diamino-2,2'-bipyridyl was placed in an atmosphere of nitrogen and then suspended in 8 mL of dry tetrahydrofuran and 3 mL of dry TEA. The suspension was stirred at room temperature for 20 min prior to adding 0.4 mL of propionyl chloride dropwise. The reaction was allowed to proceed overnight. It was then poured into 20 mL of saturated Na₂CO₃ solution and extracted four times with 40 mL of DCM. Combined organic fractions were dried over MgSO₄, and the solvent was removed on a rotary evaporator to obtain an oily residue. This residue was then dissolved in 10 mL of dry ethyl

ether and was left to crystallize in a refrigerator overnight. The solvent was decanted, and the resulting white solid was washed with an additional 10 mL of ether, followed by drying in vacuum to yield 34 mg of 4,4'-dipropionylamido-2,2'-bipyridyl. For coordination with Re(I), 40 mg of pentacarbonyl chlororhenium(I) was dissolved in 20 mL of chloroform. To that solution, 34 mg of 4,4'-dipropionylamido-2,2'-bipyridyl was added, and the reaction solution was refluxed for 3 h. The solvent was removed in vacuum, and the residual solid was dissolved in 2 mL of DCM. The solution was slowly diluted with 10 mL of diethyl ether, and the resulting solids were collected and dried in vacuum to yield 50 mg of target compound. ¹H NMR (499.75 MHz; DMSO-*d*₆) δ 11.01 (s, 2H), 8.80 (d, 2H, *J* = 6.2 Hz), 8.74 (d, 2H, *J* = 1.9 Hz), 7.74 (dd, 2H, *J* = 6.2 Hz, 1.9 Hz), 2.09 (m, 4H), 1.13 (t, 6H, *J* = 7.5 Hz). ¹³C NMR (125.67 MHz, DMSO-*d*₆): δ 174.18, 156.03, 153.61, 148.74, 115.84, 111.53, 29.83, 8.90.

UV–visible spectra of the synthesized Re(I) compounds in DMF were obtained on a Cary 50 Bio spectrophotometer. Emission spectra of the synthesized Re(I) compounds in DMF were collected on a Cary Eclipse fluorescence spectrometer. Electrochemical studies were carried out using a PAR model VersaSTAT 4 potentiostat using a single compartment cell and using 0.1 M TBAH as the supporting electrolyte in DMF at a scan rate of 100 mV/s. The electrodes used were a Pt counter electrode (~6 cm platinum wire, BASi), a glassy carbon working electrode (3.0 mm diameter, BASi), and a saturated KCl Ag/AgCl reference electrode (PAR). Ferrocene (Fc) was used as the internal standard, and all potentials were converted versus Fc/Fc⁺. DMF-saturated Ar was bubbled for 20 min through the electrochemical cell before every scan.

2.3. Surface Immobilization of Re-L1 on Silica Nanoparticles. Prior to surface immobilization of Re-L1, 150 mg of silica (SiO₂) was dried at 120 °C for 1 h and dispersed in 30 mL of dry toluene using ultrasonication. Next, 90 μL of APTMS was added to the toluene solution under constant stirring. The resulting mixture was refluxed for 12 h. The functionalized SiO₂ was then washed with excess amounts of toluene, diethyl ether, and DCM prior to further derivatization. In a separate solution, 75 mg of 2,2'-bipyridine-4,4'-dicarboxylic acid was refluxed under nitrogen in 10 mL of SOCl₂ for 6 h and dried under vacuum to remove excess SOCl₂ and any generated amounts of HCl or SO₂. The resulting product, 4,4'-bis(chlorocarbonyl)-2,2'-bipyridine, was dissolved in 30 mL of dry DCM and added dropwise to the functionalized SiO₂ dispersed in 30 mL of dry DCM and subsequently refluxed for 12 h. The product was washed with excess DCM and diethyl ether and redispersed in toluene. To this toluene solution, 30 mg of pentacarbonyl chlororhenium(I) was added, and the mixture was refluxed overnight. The final product was washed with toluene, diethyl ether, and DCM and air-dried overnight. The resulting sample in powder form is denoted Re-L1-SiO₂. The amount of Re(I) centers in Re-L1-SiO₂ was determined by elemental analysis to be 2.9 μmol per 10 mg of powder material.

Elemental analysis of the synthesized powder materials was conducted by acid digestion of the surface-immobilized Re(I) samples, followed by quantification using a Varian Vista AX induced coupled plasma atomic emission spectrometer. UV–visible spectra of powder samples pressed on BaSO₄ pellets were obtained on a Cary 50 Bio spectrophotometer fitted with a Barreliño diffuse reflectance probe using BaSO₄ as a standard. Infrared spectra of the surface-immobilized Re(I) samples were

collected on a Nicolet 6700 FTIR spectrometer equipped with a Harrick Praying Mantis diffuse reflectance accessory, a three-window chamber, and a DTGS detector.²⁸ EPR spectra were collected at room temperature on an X-band (9.5 GHz) Bruker EleXsys E-500 cw-EPR/ENDOR spectrometer. In FTIR and EPR studies of Re-L1-SiO₂ in solid state, visible-light irradiation ($\lambda > 425$ nm) was provided using a Fiber-Lite series 180 illuminator. An optical fiber was used to guide light irradiation to reach the sample through a KBr window of the photoreactor chamber.

2.4. Photocatalytic Testing. Typically, 4.0 μmol of a homogeneous Re(I) complex or 10 mg of a surface-immobilized Re(I) catalyst was dispersed in 4.0 mL of a DMF-TEOA (3:1 v/v) solution in a Pyrex test tube (8 mm diameter, 8.3 mL volume). In some tests, 4.0 μmol of Ru(bpy)₃²⁺ was added to the reaction solution for photocatalysis under visible-light irradiation. Prior to photocatalytic testing, the reaction solution was bubbled with DMF-saturated CO₂ (99.999%, Airgas) for 20 min. The reaction solution was then irradiated with an ozone-free Xe lamp equipped with a water filter (10 cm in length). In this study, an AM 1.5 filter was used with the Xe lamp to provide simulated solar irradiation. The AM 1.5 filter blocks $\sim 50\%$ of the infrared irradiation but does not significantly alter the UV or visible region in the output of the Xe lamp. A 475-nm long-pass filter was used together with the same Xe lamp to provide visible-light irradiation for the experiments with Ru(bpy)₃²⁺ as a photosensitizer. Light intensity on the reaction solution was fixed at 25 mW/cm². The head space above the reaction solution was sampled with a gastight syringe at different time intervals for product analysis using an Agilent 7820 GC equipped with a TCD detector and a 60/80 Carboxen-1000 packed column (Supelco). The turnover number (TON) was calculated as the number of moles of CO produced per mole of Re catalyst used. The amount of formic acid as a minor product of Re(I)-mediated CO₂ reduction was not monitored in this study.

3. RESULTS AND DISCUSSION

3.1. Photocatalytic CO₂ Reduction Using Homogeneous Re(I) Compounds. The amide-derivatized Re(I) compounds, Re-L1 and Re-L2 (see Scheme 1 for structures), were characterized with a variety of techniques. The MLCT band of Re-L1 has a maximum absorption at 396 nm relative to 369 nm for that of Re-bpy (Table 1), indicating a red shift of 27 nm due to derivatization of the bpy ligand with strong electron-withdrawing –CONH groups. Such derivatization also resulted

Table 1. Spectroscopic and Electrochemical Properties of Synthesized Homogeneous Re(I) Complexes

compounds	MLCT λ_{max}^a nm	em. λ_{max}^b nm	ν (CO) ^c cm ⁻¹	E_{red}^d V vs Fc/Fc ⁺
Re-bpy	369 (3.64)	611	1893, 1917, 2019	-1.78, -2.20
Re-L1	396 (4.06)	650	1897, 1920, 2020	-1.53, -1.95
Re-L2	365 (5.47)	589	1888, 1912, 2016	-1.91, -2.25

^aMaximum absorption wavelength of the MLCT band; extinction coefficients in 10³ dm³ mol⁻¹ cm⁻¹ are listed in parentheses. ^bMaximum emission wavelength of the Re(I) complexes. ^cVibrational frequencies of Re carbonyl groups; spectra collected in DMF. ^dFirst and second reduction potentials under Ar.

in a red shift of 39 nm in the emission band as well as a shift of +0.25 mV in redox potentials (Table 1). In addition, the ν (CO) bands of Re-L1 were observed at higher frequencies than those of Re-bpy (Table 1). The opposite trend was observed for Re-L2, in which the bpy ligand of the Re(I) complex was derivatized with weak electron-donating amide groups (–NHCO). In particular, both the MLCT band and emission band were slightly blue-shifted in the presence of the electron-donating groups, while the redox potentials were shifted to more negative values (Table 1). Because of the electron-donating effect of the –NHCO groups, the ν (CO) bands of Re-L2 were seen at lower frequencies than those of Re-bpy (Table 1). This is consistent with prior studies by others. For example, Koike et al. synthesized Re(I) catalysts bearing electron-donating (–CH₃) and electron-withdrawing (–CF₃) groups on the bpy ligand.¹⁴ Upon derivatization with a –CH₃ group, the first redox potential of the Re(I) catalyst was shifted by –0.12 mV and the quantum yield of CO formation was slightly increased.¹⁴ Derivatization of the Re(I) catalyst with –CF₃ group shifted the first redox potential from –1.43 to –1.03 V versus Ag/AgCl (0.1 M) and significantly lowered the quantum yield of CO formation in photocatalytic CO₂ reduction.¹⁴

The three Re(I) compounds were tested in photocatalytic CO₂ reduction using TEOA as the sacrificial electron donor under simulated solar irradiation. The presence of the electron-withdrawing –CONH groups significantly lowered the photocatalytic activity of the tricarbonyl Re(I) catalyst (Figure 1).

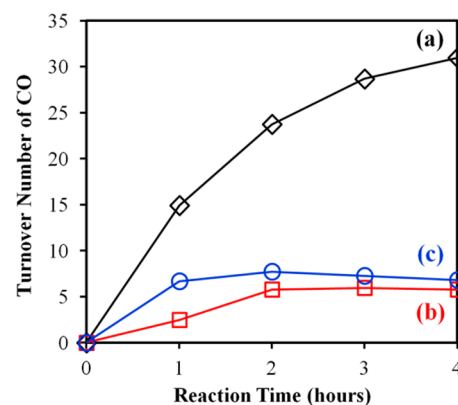


Figure 1. Photocatalytic CO₂ reduction using 1 mM (a) Re-bpy, (b) Re-L1, and (c) Re-L2 under simulated solar irradiation in a DMF-TEOA (3:1 v/v) solution.

When Re-L1 was used in photocatalysis, the TON of CO formation was 5.8, in comparison with 31 using Re-bpy after light irradiation for 4 h. This observation is consistent with the positive shift of the reduction potentials and subsequently lower reducing power of Re-L1 relative to Re-bpy. In our study, derivatization of the bpy ligand with an electron-donating –NHCO group was also detrimental to photocatalytic reactivity of the Re(I) catalyst. Under the same experimental conditions, a TON of 6.8 was obtained using Re-L2 as the photocatalyst. The homogeneous Re-L1 and Re-L2 became inactive after the first 2 h of photocatalysis (Figure 1), possibly due to altered photophysical properties, poor stability of the derivatized Re(I) complexes under the experimental conditions, or both.

The synthesized Re(I) complexes were also tested in photocatalytic CO₂ reduction in the presence of Ru(bpy)₃²⁺,

which functioned as a photosensitizer to harvest visible light ($\lambda > 475$ nm) and transfer electrons to the Re(I) catalysts upon excited-state quenching by TEOA. The Re(I) catalysts do not have significant absorption in the visible-light ($\lambda > 475$ nm) region. In the presence of $\text{Ru}(\text{bpy})_3^{2+}$, TONs of 15 and 4.8 were obtained for Re-bpy and Re-L2, respectively, after visible-light irradiation for 4 h (Figure 2). In contrast, the combination

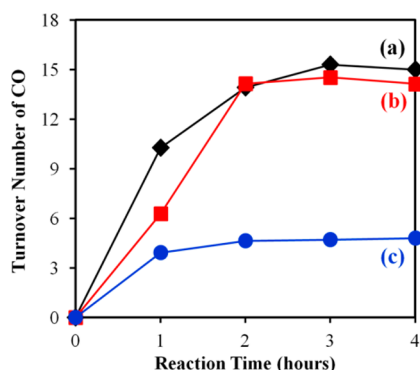


Figure 2. Photocatalytic CO_2 reduction using 1 mM (a) Re-bpy, (b) Re-L1, and (c) Re-L2 under visible-light ($\lambda > 475$ nm) irradiation in the presence of 1 mM $\text{Ru}(\text{bpy})_3^{2+}$ in a DMF-TEOA (3:1 v/v) solution.

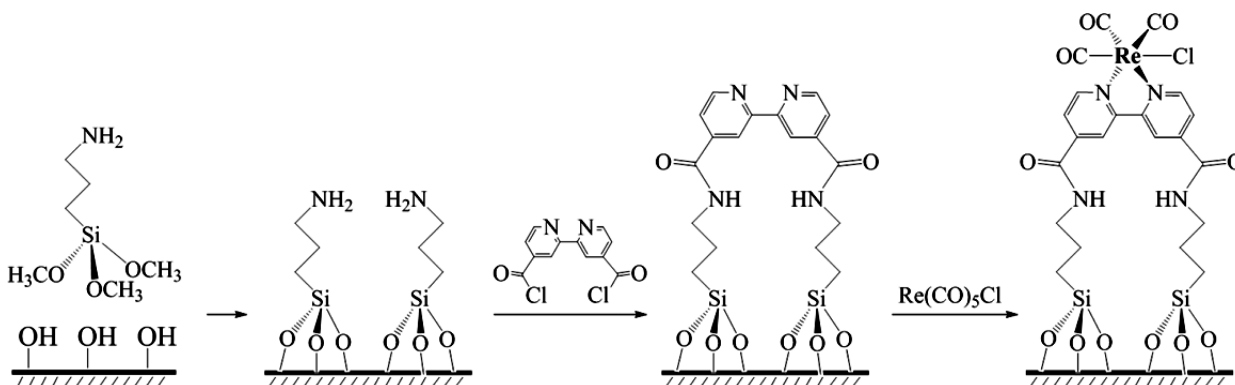
of $\text{Ru}(\text{bpy})_3^{2+}$ and Re-L1 resulted in a TON of 14 upon visible-light irradiation (Figure 2). Since Re-L1 showed lower photocatalytic activity than Re-bpy or Re-L2 upon direction MLCT excitation (Figure 1), the comparison shown in Figure 2 suggests that electron transfer between $\text{Ru}(\text{bpy})_3^{3+}$ and Re-L1 is much more efficient than that between $\text{Ru}(\text{bpy})_3^{3+}$ and Re-bpy or Re-L2. Such a difference might be due to the presence of strong electron-withdrawing groups ($-\text{CONH}$) in Re-L1, although the $-\text{CONH}$ groups were associated with the relatively lower photocatalytic activity of Re-L1 in comparison Re-bpy (see Figure 1). The red shift in the MLCT band and enhanced absorption in the visible-light region of Re-L1 relative to Re-bpy and Re-L2 (Table 1) might also contribute to the difference in photocatalytic activity shown in Figure 2. It should be noted that different photon sources were used to obtain the results shown in Figures 1 and 2. Therefore, the comparison described here does not reflect the effect of $\text{Ru}(\text{bpy})_3^{2+}$ photosensitization on the CO_2 -reduction activity of individual Re catalysts, which is not the focus of this present study.

3.2. Synthesis and Characterization of Surface-Immobilized Re(I) Compounds. Tricarbonyl Re(I) com-

plexes have been covalently attached to solid-state nanostructures, including titanium dioxide,²⁹ silica,³⁰ and a polyoxometalate,³¹ for photochemical and spectroscopic studies. The Re(I) complexes were also incorporated in light-absorbing metal-organic framework³² and periodic mesoporous organosilica³³ for enhanced photocatalytic CO_2 -to- CO conversion. Silica nanomaterials have been widely utilized as solid-state support for photocatalysts.^{34,35} In this study, surface immobilization of both Re-L1 and Re-L2 on a fumed silica was attempted via a route different from that in our previous study.²⁴ Scheme 2 shows the synthesis of Re-L1 immobilized on the surface of SiO_2 ("Re-L1- SiO_2 "). In this approach, the silica surface containing abundant silanol groups was initially functionalized with APTMS, a silane coupling agent bearing an amine group. The functionalized surface was further derivatized by reacting with 4,4'-bis(chlorocarbonyl)-2,2'-bipyridine prior to coordination of Re(I) with the bpy moieties on the surface (Scheme 2). This synthetic route has the advantage of forming a monolayer of Re(I) catalytic sites that are covalently linked to the surface through a few chemical bonds. As mentioned earlier in the Experimental Section, the amount of Re(I) centers in Re-L1- SiO_2 was determined by elemental analysis to be 2.9 μmol per 10 mg of powder material, corresponding to a surface density of ~ 0.9 Re(I) per square nanometer. This surface density is very similar to that obtained in our previous study using a different synthetic approach and a different solid-state support.²⁴

Surface immobilization of Re-L2 on SiO_2 was also attempted but failed to produce the target material denoted Re-L2- SiO_2 . A key step in the synthesis of Re-L2- SiO_2 involved the reaction between surface ester groups and 4,4'-diamino-2,2'-bipyridine prior to coordination with Re(I). The infrared spectrum of the synthesized Re-L2- SiO_2 (not shown) indicated the presence of a significant amount of physically adsorbed $\text{Re}(\text{NH}_2\text{-bpy})(\text{CO})_3\text{Cl}$, where $\text{NH}_2\text{-bpy}$ is 4,4'-diamino-2,2'-bipyridine. Although the amount of Re(I) centers in Re-L2- SiO_2 was determined by elemental analysis to be 1.5 μmol per 10 mg of powder material, the synthesized material resulted in TONs of CO formation less than 0.5 after photochemical CO_2 reduction for 4 h under either simulated solar irradiation or visible-light irradiation in the presence of $\text{Ru}(\text{bpy})_3^{2+}$. Most likely, the reaction between surface ester groups and 4,4'-diamino-2,2'-bipyridine did not proceed with sufficiently high yield under the synthetic condition, and the physically adsorbed $\text{Re}(\text{NH}_2\text{-bpy})(\text{CO})_3\text{Cl}$ on a silica surface was not an active photocatalyst for CO_2 reduction.

Scheme 2. Synthesis of Re-L1- SiO_2



In comparison, the successful synthesis of Re-L1-SiO₂ is well supported by spectroscopic evidence. Figure 3 shows the

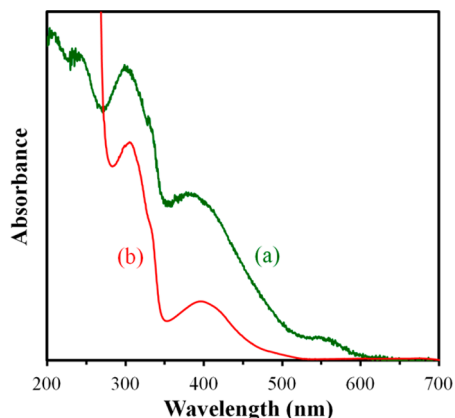


Figure 3. Optical spectra of (a) Re-L1-SiO₂ and (b) Re-L1.

optical spectra of Re-L1-SiO₂ and the homogeneous Re-L1 in the spectral region between 200 and 700 nm. The two major features in the spectrum of Re-L1, one around 300 nm ($\pi\pi^*$ transition of bpy) and the other around 400 nm (the MLCT band), are clearly seen in the spectrum of Re-L1-SiO₂. A relatively weak absorption around 550 nm is also present in the spectrum of Re-L1-SiO₂ (Figure 3b). This band might be associated with a trace amount of Fe-bpy species introduced during the synthesis of Re-L1-SiO₂.

Infrared results further prove that in Re-L1-SiO₂, the Re(I) catalyst is covalently attached to the surface via the -CONH amide linkage. The following characteristics are noticed in the FTIR spectrum of Re-L1-SiO₂ shown in Figure 4a: (i) the

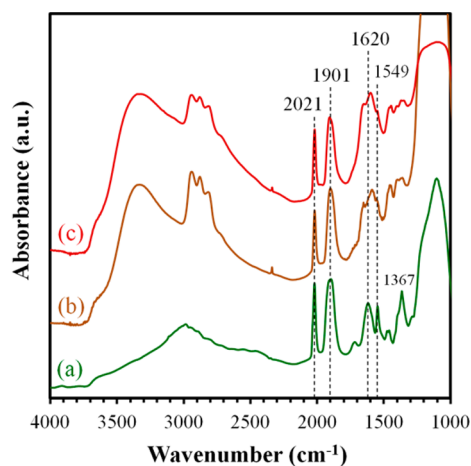


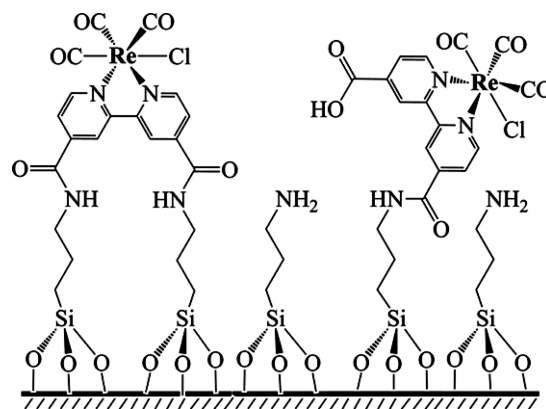
Figure 4. FTIR spectra of Re-L1-SiO₂: (a) before photocatalytic testing, (b) after photocatalytic testing under simulated solar irradiation, and (c) after photocatalytic testing under visible-light irradiation in the presence of Ru(bpy)₃²⁺. Photocatalytic testing was carried out in a mixture of DMF-TEOA (volume ratio 3:1) for 4 h.

absence of silanol groups, which are usually observed at 3745 cm⁻¹, as a result of surface functionalization with APTMS; (ii) the presence of Re-carbonyl bands at 2021 and 1901 cm⁻¹; and (iii) the presence of absorptions associated with the amide linkage at ~1620, 1549 (N-H bend), and 1367 cm⁻¹ (C-N stretch). In our previous work,²⁴ the C=O stretching band of the same amide linkage was observed at 1657 cm⁻¹. In this

present study, the absorption at ~1620 cm⁻¹ shown in Figure 4a is likely a result of two overlapping absorptions: the C=O stretching band at 1657 cm⁻¹ and the N-H bending band of surface amine groups around 1600 cm⁻¹. These two overlapping absorptions are more clearly seen in the spectra of Re-L1-SiO₂ after photocatalysis shown in Figure 4b and 4c.

In addition, two less-intense peaks at ~1720 and ~1460 cm⁻¹ (not labeled), are present in the spectrum shown in Figure 4a. The peaks around 1720 and 1460 cm⁻¹ are likely due to the presence of carboxylic and carboxylate groups, respectively, on the functionalized silica surface. Therefore, the spectrum shown in Figure 4a suggests that not all of the surface amine groups were consumed in the reaction with 4,4'-bis(chlorocarbonyl)-2,2'-bipyridine following the synthesis described in Scheme 2. Furthermore, the presence of two peaks around 1720 and 1460 cm⁻¹ in Figure 4a implies that a relatively small amount of 4,4'-bis(chlorocarbonyl)-2,2'-bipyridine was covalently attached on the silica surface through the one-arm (one -CONH linkage) configuration instead of the intended two-arm mode. However, our spectroscopic (optical and infrared) results shown in Figures 3 and 4a indicate that most of the surface-immobilized Re(I) units have the target structure of Re-L1-SiO₂. Scheme 3 shows the structures of coexisting surface functionalities, including free amine groups, one-arm Re(I) sites, and the target two-arm Re(I) sites, in the synthesized material.

Scheme 3. Possible Surface Sites on the Functionalized Silica Nanoparticles, Including the Target Two-Arm Re-L1-SiO₂, Free Amine Groups and the One-Arm Re(I) Complex



The synthesized Re-L1-SiO₂ in powder form was tested in photocatalytic CO₂ reduction. A TON of 6.9 was obtained using Re-L1-SiO₂ as the photocatalyst after 4 h under simulated solar irradiation, whereas a TON of 11 was obtained when Re-L1-SiO₂ was tested under visible-light irradiation in the presence of Ru(bpy)₃²⁺ as a photosensitizer (Figure 5). Therefore, the activity of Re-L1-SiO₂ was comparable to the homogeneous Re-L1.

Similar to the homogeneous Re-L1, the heterogeneous Re-L1-SiO₂ became less active after the first 2 h of reaction under the experimental conditions (Figure 5). In the study by Takeda et al., deactivation of a surface-immobilized Re(I) catalyst was associated with the formation of Re-formate species, which was identified by carbonyl absorptions at 2018, 1912, and 1894 cm⁻¹.³³ In our study, infrared spectra of Re-L1-SiO₂ were collected after photocatalysis followed by thorough solvent washing. Figure 4 compares the spectrum of fresh Re-L1-SiO₂

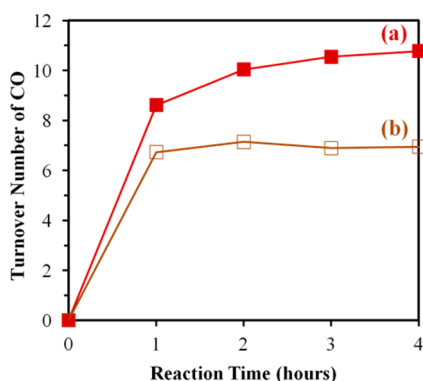


Figure 5. Photocatalytic CO₂ reduction using Re-L1-SiO₂: (a) under visible-light irradiation in the presence of Ru(bpy)₃²⁺ and (b) under simulated solar irradiation.

with the spectra of the same material after photocatalysis under different light irradiation. The Re-carbonyl bands at 2021 and 1901 cm⁻¹ in the spectra of tested samples are almost identical to those in the spectrum of fresh Re-L1-SiO₂. The spectra shown in Figure 4 indicate no significant formation of Re-formato species after Re-L1-SiO₂ was tested in photocatalytic CO₂ reduction under the experimental conditions. Therefore, the low reactivity of Re-L1-SiO₂ after the first 2 h of reaction must be associated with the performance of Re-L1 in photocatalysis, as shown in Figures 1 and 2.

3.3. In Situ Spectroscopic Studies of Re-L1-SiO₂ in Solid State. The use of a robust solid-state support for the Re(I) catalyst permits the study of Re-L1-SiO₂ with in situ FTIR and EPR spectroscopies in the absence of an organic solvent. Prior to the spectroscopic investigation, a small amount of Re-L1-SiO₂ was thoroughly mixed with a few drops of TEOA as well as KBr. Figure 6 shows the FTIR spectra of the

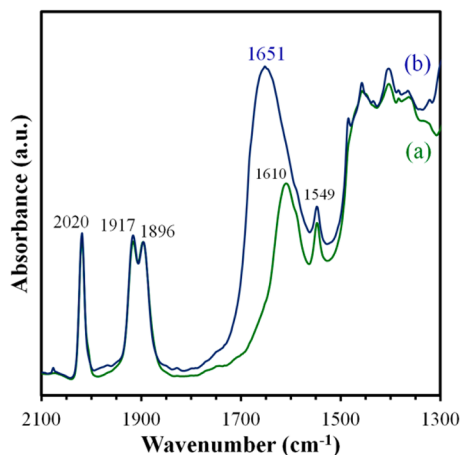


Figure 6. FTIR spectra of Re-L1-SiO₂ in solid state in the presence of (a) Ar and (b) CO₂. The sample was mixed with KBr and TEOA.

resulting mixture in the presence of Ar and CO₂. Both spectra shown in Figure 6 contain three Re-carbonyl bands at 2020, 1917, and 1896 cm⁻¹, in comparison with absorptions at 2020, 1920, and 1897 cm⁻¹ for homogeneous Re-L1 in DMF (Table 1). Only two Re-carbonyl bands at 2021 and 1901 cm⁻¹ are present in the spectrum of Re-L1-SiO₂ in the absence of TEOA (Figure 4a).

In our previous study, Re-bpy was physically adsorbed in a hierarchical mesoporous ZSM-5 zeolite and further mixed with TEOA.²⁸ The infrared spectrum of the physically adsorbed Re-bpy sample contains two broad absorption features between 1800 and 2100 cm⁻¹.²⁸ Because of direct interactions of Re-bpy with the zeolite surface, the two broad absorption features consist of multiple overlapping peaks;²⁸ therefore, the presence of three well-defined Re-carbonyl bands in the spectrum of Re-L1-SiO₂ shown in Figure 6 suggests that the surface Re(I) sites are distinct and that most surface Re(I) sites are in a coordination environment identical to that of Re-L1. The FTIR spectra shown in Figure 6 also highlight the formation of surface adsorbed bicarbonate when Re-L1-SiO₂ was exposed to CO₂ in the presence of TEOA. The bicarbonate species is associated with a broad band at 1651 cm⁻¹ (Figure 6b) characteristic of the O–C–O stretching of bidentate bicarbonate species.²⁸

The Re-L1-SiO₂ sample containing TEOA was further exposed to visible-light ($\lambda > 425$ nm) irradiation in the presence of gaseous CO₂. After light irradiation for 1 h, the three Re-carbonyl bands shifted to lower wavenumbers at 2017, 1907, and 1888 cm⁻¹ (Figure 7b), corresponding to changes of

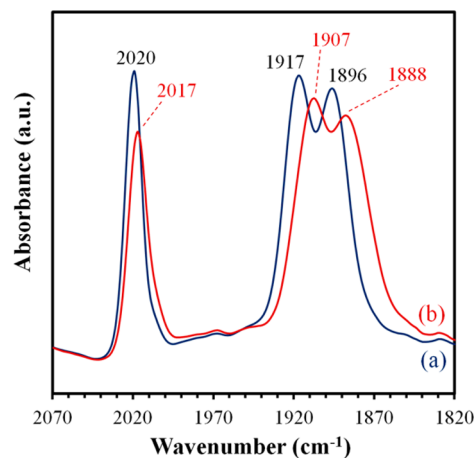


Figure 7. FTIR spectra of Re-L1-SiO₂ in solid state (a) before and (b) after visible-light ($\lambda > 425$ nm) irradiation for 1 h in the presence of CO₂. The sample was mixed with KBr and TEOA.

3, 10, and 8 cm⁻¹, respectively. We attribute the shift to bipyridine-based reduction of Re-L1-SiO₂, although previous infrared spectroelectrochemical studies reported a shift of ~ 20 cm⁻¹ due to primarily bipyridine-based reduction of the homogeneous Re-bpy.^{16,36} The much smaller shift observed in our study should be associated with the presence of electron-withdrawing amide (–CONH) substitution on the bpy ligand of Re-L1-SiO₂.

Photoinitiated bipyridine-based reduction of Re-L1-SiO₂ was further confirmed by EPR study of the same sample containing TEOA. Figure 8 shows the EPR spectra of Re-L1-SiO₂ in powder form before and after visible-light ($\lambda > 425$ nm) irradiation in the presence of gaseous CO₂. The spectra shown in Figure 8 clearly demonstrate the formation of paramagnetic species upon light irradiation. In particular, the EPR spectrum collected prior to light irradiation (Figure 8a) does not show any noticeable signal, but the EPR spectrum upon light irradiation (Figure 8b) contains resonance originating from an interaction between the unpaired electron in reduced bpy ligands with Re(I) nuclei.^{37,38} Beyond the spectroscopic

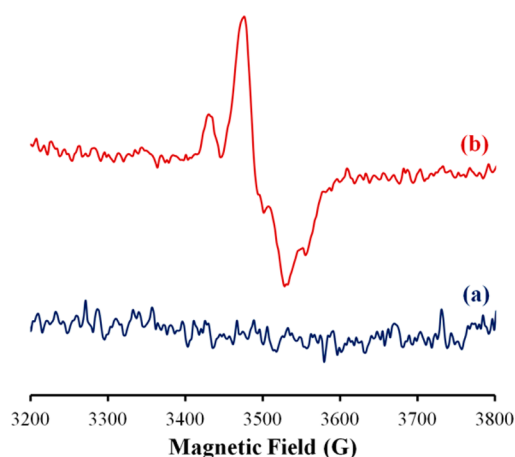


Figure 8. EPR spectra of Re-L1-SiO₂ in solid state (a) before and (b) after visible-light ($\lambda > 425$ nm) irradiation for 5 min in the presence of CO₂. The sample was mixed with KBr and TEOA. The spectra were collected at room temperature.

changes described in Figures 7 and 8, no significant change was observed in the FTIR and EPR spectra of Re-L1-SiO₂ in other spectral regions or after prolonged light irradiation.

The in situ spectroscopic studies demonstrated one-electron reduction on the bpy ligand of Re-L1-SiO₂ in solid state upon visible-light irradiation in the presence of a sacrificial electron donor. Such bipyridine-based reduction is an important step in photocatalytic CO₂ reduction using homogeneous Re(I) compounds. No significant formation of CO was observed in the infrared study under these experimental conditions. This is likely due to the lack of sufficient driving force for the reduced surface Re(I) species to acquire the second electron needed for CO₂-to-CO conversion on Re(I), which is known as a two-electron process. In this sense, photoelectrochemical CO₂ reduction using molecular catalysts attached to electrodes is among the most promising approaches for efficient CO₂ reduction. In the photoelectrochemical approach, an applied bias potential could facilitate the accumulation of two electrons on the same catalyst site and subsequently achieve efficient CO₂-to-CO conversion. Our current research involves derivatization and covalent attachment of tricarbonyl Re(I) catalysts on electrodes for use in photoelectrochemical CO₂ reduction.

4. CONCLUSIONS

Although amide bonds have been utilized as versatile linkages for building supramolecular complexes, this present study showed that derivatization of the bipyridine ligand with amide groups significantly altered the optical, electrochemical, and photocatalytic properties of tricarbonyl Re(I) catalysts. In photocatalytic CO₂ reduction, the presence of electron-withdrawing amide (–CONH) groups on the bpy ligand lowered the activity of Re(bpy)(CO)₃Cl by a factor of ~6 when the MLCT band of the Re(I) catalyst was directly excited. Such a detrimental effect disappeared in the presence of Ru(bpy)₃²⁺, which initiated the photocatalysis by absorbing visible light and subsequently transferring electrons to the Re(I) catalyst upon excited-state quenching by TEOA. Likely, the presence of electron-withdrawing amide groups facilitated intermolecular electron transfer from Ru(bpy)₃^{•+} to the Re(I) catalyst.

This study also proved that amide bonds are viable linkages to achieve robust surface immobilization of Re(bpy)(CO)₃Cl

on silica nanoparticles. The surface-immobilized Re(I) complex demonstrated optical and photocatalytic properties very similar to the homogeneous Re(I) compound bearing the electron-withdrawing amide groups. The use of photochemically inert silica support permitted the study of structural and functional characteristics of the Re(I) catalyst by using in situ spectroscopic techniques. Our in situ spectroscopic studies revealed that the coordination environment of the Re(I) centers was conserved after surface immobilization and that the surface Re(I) sites were well separated. In addition, visible-light irradiation resulted in bipyridine-based one-electron reduction of the surface Re(I) catalyst, an important step in photocatalytic CO₂ reduction mediated by homogeneous Re(I) compounds.

AUTHOR INFORMATION

Corresponding Author

*E-mail: gonghu.li@unh.edu.

Notes

The authors declare no competing financial interest.

ACKNOWLEDGMENTS

This paper is dedicated to the 40-year anniversary of Hubei Normal University. This research was supported by the National Science Foundation through the Nanoscale Science & Engineering Center for High-Rate Nanomanufacturing (NSF EEC 0832785). The generous donation of Aerosil 200 by Evonik is greatly appreciated. We are grateful to Dr. N. Dennis Chasteen, Dr. Sterling Tomellini, Dr. Edward Wong, Dr. Roy Planalp, Dr. Kevin Gardner, and Scott Greenwood for helpful discussions and assistance in various aspects of the experiments.

REFERENCES

- Arakawa, H.; Aresta, M.; Armor, J. N.; Barteau, M. A.; Beckman, E. J.; Bell, A. T.; Bercaw, J. E.; Creutz, C.; Dinjus, E.; Dixon, D. A.; Domen, K.; DuBois, D. L.; Eckert, J.; Fujita, E.; Gibson, D. H.; Goddard, W. A.; Goodman, D. W.; Keller, J.; Kubas, G. J.; Kung, H. H.; Lyons, J. E.; Manzer, L. E.; Marks, T. J.; Morokuma, K.; Nicholas, K. M.; Periana, R.; Que, L.; Rostrup-Nielsen, J.; Sachtler, W. M. H.; Schmidt, L. D.; Sen, A.; Somorjai, G. A.; Stair, P. C.; Stults, B. R.; Tumas, W. *Chem. Rev.* **2001**, *101*, 953–996.
- Mikkelsen, M.; Jorgensen, M.; Krebs, F. C. *Energy Environ. Sci.* **2010**, *3*, 43–81.
- Kumar, B.; Llorente, M.; Froehlich, J.; Dang, T.; Sathrum, A.; Kubiak, C. P. *Annu. Rev. Phys. Chem.* **2012**, *63*, 541–569.
- Cole, E. B.; Bocarsly, A. B. In *Carbon Dioxide as Chemical Feedstock* Aresta, M., Ed.; Wiley-VCH Verlag GmbH & Co. KGaA: Weinheim, 2010; pp 291–316.
- Crabtree, R. H. In *Energy Production and Storage: Inorganic Chemical Strategies for a Warming World* Crabtree, R. H., Ed.; John Wiley & Sons, Ltd.: New York, 2010; pp 301–306.
- Dimitrijevic, N. M.; Vijayan, B. K.; Poluektov, O. G.; Rajh, T.; Gray, K. A.; He, H.-Y.; Zapol, P. J. *Am. Chem. Soc.* **2011**, *133*, 3964–3971.
- Mori, K.; Yamashita, H.; Anpo, M. *RSC Adv.* **2012**, *2*, 3165–3172.
- He, H.; Liu, C.; Dubois, K. D.; Jin, T.; Louis, M. E.; Li, G. *Ind. Eng. Chem. Res.* **2012**, *51*, 11841–11849.
- Morris, A. J.; Meyer, G. J.; Fujita, E. *Acc. Chem. Res.* **2009**, *42*, 1983–1994.
- Takeda, H.; Koike, K.; Morimoto, T.; Inumaru, H.; Ishitani, O. *Adv. Inorg. Chem.* **2011**, *63*, 137–186.
- Agarwal, J.; Johnson, R. P.; Li, G. *J. Phys. Chem. A* **2011**, *115*, 2877–2881.
- Hawecker, J.; Lehn, J.-M.; Ziessel, R. *J. Chem. Soc., Chem. Commun.* **1983**, 536–538.

- (13) Worl, L. A.; Duesing, R.; Chen, P.; Ciana, L. D.; Meyer, T. J. *J. Chem. Soc., Dalton Trans.* **1991**, 849–858.
- (14) Koike, K.; Hori, H.; Ishizuka, M.; Westwell, J. R.; Takeuchi, K.; Ibusuki, T.; Enjouji, K.; Konno, H.; Sakamoto, K.; Ishitani, O. *Organometallics* **1997**, *16*, 5724–5729.
- (15) Takeda, H.; Koike, K.; Inoue, H.; Ishitani, O. *J. Am. Chem. Soc.* **2008**, *130*, 2023–2031.
- (16) Smieja, J. M.; Kubiak, C. P. *Inorg. Chem.* **2010**, *49*, 9283–9289.
- (17) Windle, C. D.; Campian, M. V.; Duhme-Klair, A.-K.; Gibson, E. A.; Perutz, R. N.; Schneider, J. *Chem. Commun.* **2012**, 48, 8189–8191.
- (18) Gabriellsson, A.; Lindsay, S. J. R.; Perutz, R. N. *Dalton Trans.* **2008**, 4259–4269.
- (19) Schneider, J.; Vuong, K. Q.; Calladine, J. A.; Sun, X.-Z.; Whitwood, A. C.; George, M. W.; Perutz, R. N. *Inorg. Chem.* **2011**, *50*, 11877–11889.
- (20) Kiyosawa, K.; Shiraiishi, N.; Shimada, T.; Masui, D.; Tachibana, H.; Takagi, S.; Ishitani, O.; Tryk, D. A.; Inoue, H. *J. Phys. Chem. C* **2009**, *113*, 11667–11673.
- (21) Li, G.; Sproviero, E. M.; McNamara, W. R.; Snoeberger, R. C. I.; Crabtree, R. H.; Brudvig, G. W.; Batista, V. S. *J. Phys. Chem. B* **2010**, *114*, 14214–14222.
- (22) McNamara, W. R.; Snoeberger, R. C. I.; Li, G.; Schleicher, J. M.; Cady, C. W.; Poyatos, M.; Schmuttenmaer, C. A.; Crabtree, R. H.; Brudvig, G. W.; Batista, V. S. *J. Am. Chem. Soc.* **2008**, *130*, 14329–14338.
- (23) Sek, S.; Palys, B.; Bilewicz, R. *J. Phys. Chem. B* **2002**, *106*, 5907–5914.
- (24) Dubois, K.; He, H.; Liu, C.; Vorushilov, A. S.; Li, G. *J. Mol. Catal. A: Chem.* **2012**, 363–364, 208–213.
- (25) Barton, E. E.; Rampulla, D. M.; Bocarsly, A. B. *J. Am. Chem. Soc.* **2008**, *130*, 6342–6344.
- (26) Smieja, J. M.; Benson, E. E.; Kumar, B.; Grice, K. A.; Seu, C. S.; Miller, A. J. M.; Mayer, J. M.; Kubiak, C. P. *Proc. Natl. Acad. Sci. U.S.A.* **2012**, *109*, 15646–15650.
- (27) Yao, S. A.; Ruther, R. E.; Zhang, L.; Franking, R. A.; Hamers, R. J.; Berry, J. F. *J. Am. Chem. Soc.* **2012**, *134*, 15632–15635.
- (28) Dubois, K.; Petushkov, A.; Cardona, E. G.; Larsen, S. C.; Li, G. *J. Phys. Chem. Lett.* **2012**, *3*, 486–492.
- (29) Anfuso, C. L.; Snoeberger, R. C., III; Ricks, A. M.; Liu, W.; Xiao, D.; Batista, V. S.; Lian, T. *J. Am. Chem. Soc.* **2011**, *133*, 6922–6925.
- (30) Rosenfeld, D. E.; Gengeliczki, Z.; Smith, B. J.; Stack, T. D. P.; Fayer, M. D. *Science* **2011**, *334*, 634–639.
- (31) Zhao, C.; Huang, Z.; Rodríguez-Córdoba, W.; Kambara, C. S.; O'Halloran, K. P.; Hardcastle, K. L.; Musaev, D. G.; Lian, T.; Hill, C. L. *J. Am. Chem. Soc.* **2011**, *133*, 20134–20137.
- (32) Wang, C.; Xie, Z.; deKrafft, K. E.; Lin, W. *J. Am. Chem. Soc.* **2011**, *133*, 13445–13454.
- (33) Takeda, H.; Ohashi, M.; Tani, T.; Ishitani, O.; Inagaki, S. *Inorg. Chem.* **2010**, *49*, 4554–4559.
- (34) Frei, H. *Chimia* **2009**, *63*, 721–730.
- (35) Kibombo, H. S.; Peng, R.; Rasalingam, S.; Koodali, R. T. *Catal. Sci. Technol.* **2012**, *2*, 1737–1766.
- (36) Johnson, F. P. A.; George, M. W.; Hartl, F.; Turner, J. J. *Organometallics* **1996**, *15*, 3374–3387.
- (37) Kaim, W.; Kohlmann, S. *Chem. Phys. Lett.* **1987**, *139*, 365–369.
- (38) Scheiring, T.; Klein, A.; Kaim, W. *J. Chem. Soc., Perkin Trans. 2* **1997**, 2569–2571.